Anonymous Referee #1

This study investigates the incorporation of coarse and giant desert dust particles (with diameter greater than 20 μm) in the WRF model, together with the GOCART aerosol model and the AFWA dust emission scheme. The authors implemented a number of extensions to the original model. More specifically, they used a prescribed dust particle size distribution for emitted dust particles at the source based on in situ measurements from the FENNEC campaign and employed 5 size bins with diameters up to 100 μm (corresponding to giant particles). Moreover, they implemented an updated drag coefficient that applies to the above bins and is representative of high values of Re number. The simulations were performed from 29 July to 25 August 2015. The model output were validated against various observational datasets.

The article is well written and promotes the research in the modelling of the desert dust. The use of English is excellent and the conclusions are supported by the results. It is suggested to accept this article for publication after some minor corrections are performed.

The recognition of our work from the reviewer is much appreciated. We would like to thank him/her for taking the necessary time and effort to review our manuscript. We sincerely appreciate all your valuable comments and suggestions. The manuscript has been revised considering all the suggestions raised by the reviewer.

Suggested corrections:

Section 2.1.3: please include a) whether the vertical levels (line 220) were defined by WRF or by the authors (providing how you chose them in the latter case), b) which UTC time was chosen for the original initialization/each re-initialization (line 221), c) some more detailed information about the model results that you used from each 84 hour run (i.e. whether you removed the first 12 hours of each run due to model spin-up and utilized the rest; line 221), d) the topography and land-use datasets, e) whether the sea-surface temperatures were updated from GFS-FNL analyses every 72 hours at the initial time of each run or every 6 hours together with the lateral boundary conditions.

We agree with this comment and we have incorporated the reviewer's suggestion throughout Section 2.1.3, explaining that the specific heights of the vertical levels are defined by the model. The sea surface temperatures in the model acquired by the NCEP daily SST analysis (RTG_SST_HR) are updated every six hours along with the lateral boundary conditions. Each 84-hour run was initialized at 12 UTC and the first 12 hours were removed accounting for the model spin-up. Topography is interpolated from the 30s Global Multi-resolution Terrain Elevation Data 2010 (GMTED2010, Danielson and Gesch, (2011)). We use land-data based on Moderate-resolution Imaging Spectroradiometer (MODIS) observational data modified by the University of Boston (Gilliam and Pleim, 2010). Hence based on our reply we modified the Sect 2.1.3 of the original manuscript (line 216, page 8):

"Using the WRF-L code, we first run the CONTROL experiment. Our simulation period coincides with the AER-D experimental campaign (29/7 - 25/8/2015) for a domain bounded between the 1.42°N and 39.99°N parallels and stretching between the 30.87°W and 46.87°E meridians (Fig. 3). The simulation area encompasses the major Saharan sources also including the downwind areas in the eastern Tropical Atlantic. We use an equal-distance grid with a spatial grid spacing of 15 km x 15 km consisting of 550 × 300 points whereas in vertical, 70 vertical sigma pressure levels up to 50 hPa are utilized. The simulation period consists of nine 84-hour forecast runs, which are initialized at 12 UTC, using the 6-hour Global Forecast System Final Analysis (GFS - FNL) reanalysis product, available at a 0.25°x0.25° spatial resolution. The sea surface temperatures, acquired by the NCEP daily global SST analysis (RTG_SST_HR), are updated every six hours along with the lateral boundary conditions. From each 84-hour cycle, the first 12 hours are discarded due to model spin up. Likewise, the first week of the simulation served as a spin-up run for the accumulation of the background dust loading and it is excluded from the analysis."

Line 369-373: Have you validated the simulated upper air wind field, e.g. using ERA5? Western Africa is characterized by a complex wind regime. There is a large area with pink colors (i.e. dust) in area B of Figure 7f. Therefore, the dust errors may be also due to erroneous wind field.

The reviewer raises an important issue regarding how a possible wind speed bias can affect the emission. Menut, (2008) quantified the impact of the meteorological data forcing (using either NCEP or ECMWF as initial/boundary conditions) above Sahara sources and reported that the difference between the two emission fluxes can reach a factor of 3. Moreover, they noted that this difference is not systematic and no conclusion was made of which dataset overperforms. Following the reviewer's suggestion, we performed a validation analysis of the WRF-L upper wind fields (i.e., at 300 and 500 hPa) versus ERA5, both reprojected at a common grid (0.25 x 0.25 spatial resolution).The obtained results for the two pressure levels, on 5th August 2015 at 00 UTC, are illustrated in the Figure below. It is evident that the two models produce similar meteorological patterns with deviations only on the wind speeds. Focusing on the latitudinal band (10-25°N) where the Saharan dust is transported over the Tropical Atlantic Ocean, mainly positive WRF-ERA5 declinations are recorded over the W. Sahara while the opposite is revealed over the outflow regions. This differences in the two models above land are almost consistent throughout the whole simulation. In terms of magnitude lie mostly in the range of 2-8 m/s (in absolute terms) at 500 hPa and they are slightly higher at 300 hPa.

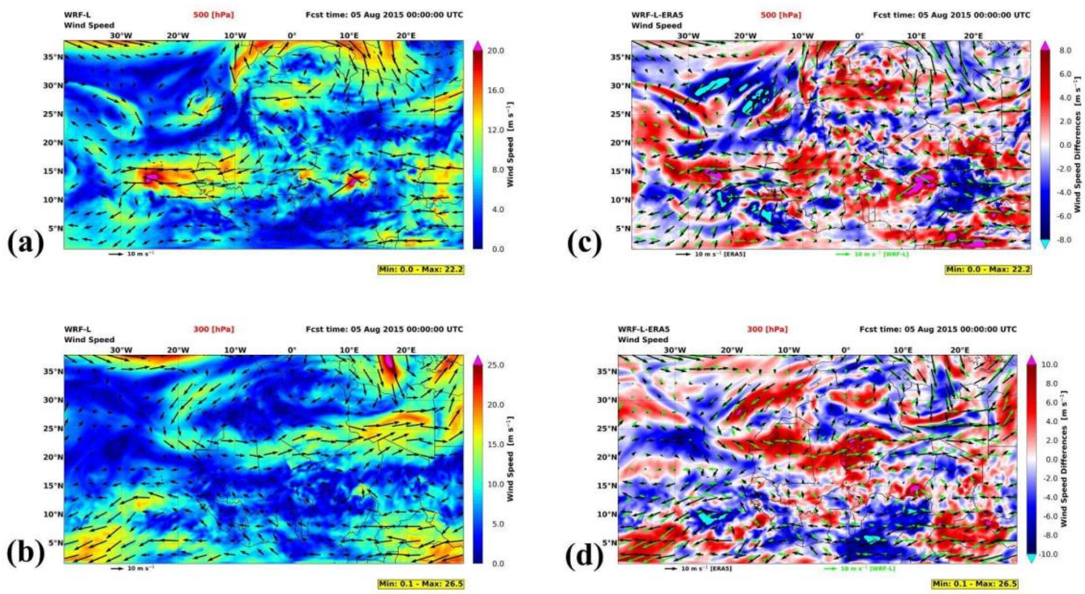

Figure R1: WRF-L wind fields at (a) 500 and (b) 300 hPa, and wind speed differences with respect to ERA5 wind fields at (c) 500hPa and (d) at 300 hPa.

Deviations in the wind fields can impact both the emission and the transport of dust. The link between winds and produced emissions and transport is rather a complex issue and needs a more thorough investigation, which is beyond the scope of this article. More specifically, regarding the accuracy of the atmospheric models' forecasts, among the possible reasons could be the induced uncertainties in the wind fields of the global datasets, which are used as initial and boundary conditions. In the global datasets, the assimilation of observations and measurements assists models in reducing their errors. Please note that according to RC3 reviewer comments, to avoid any confusion in the reader, the part related to Fig. 7 of the original manuscript has been removed.

Technical corrections:

Line 23: "… diameters of 5.5-17 μm …"

Done.

Line 129: "… are shown in Table 1."

Done.

In equation 5, C_D must be replaced by C_D/C_{cun} (following the terms of equation 4) or by the equivalent $C_{D,slip}$ of equation 11.

We agree. We have, accordingly, revised the whole Section 2.1.2, which includes Eq.5. The revised equation 5 is now given by Eq. 6 in line XX, p.XX. The revised Section 2.1.2 is included in lines 171, page 6:

"The constant velocity that a particle builds up falling vertically within the Earth's atmosphere, is defined as the terminal settling velocity u_{term}, and it can be estimated by solving the 1-D equation of motion at the steady state limit, where net force is assumed to be equal to zero:

$$\rho_p \cdot V_p . g = \frac{1}{2} \cdot \frac{C_D}{C_{cun}} \cdot A_p \cdot \rho_{air} \cdot u_{term}^2, \qquad (6)"$$

Line 178: the units of μ should be kg m-1 s-1 so that equation 9 to be unit less.

Done

Line 180: please correct the numerator of μ (i.e. 1.4.58).

Done

Line 182: "Equation 8 has been derived …".

Done.

Line 183: "… Davies (1945) …".

Done

Line 184: "… drag coefficient becomes:".

Done

Line 193: "… Substituting Eq. 6-9 in Eq. 5 …".

Done

Line 197: "… Stoke's Law (Eq. 11) …".

Done

Line 200: "… of Eq. 14, proposed …".

Done

Line 226: please include the full name of DOD (Dust Optical Depth) at its first appearance in the article.

Done

Line 339: Ryder et al. (2013a) or (2013b)?

It is Ryder et al. (2018)

Line 367: "… and the MIDAS DOD …".

Done

Line 385: " … as shown in Fig. 5."

Done

Line 391: "… for bin 5 (40-100 μm)."

Done

Line 397 and 833-834: What is the domain of interest? Were the results averaged in the whole model domain of figure 3 from 5 to 25 August 2015?

We would like to thank the reviewer for pointing this out. We agree with this comment. Therefore, we have revised the manuscript so as to emphasize this point. This study coincides with the AER-D field campaign. The most activated dust sources that affected the vicinity of Cape Verde were located in the west coast of Africa, Mali, Mauritania, Maroco, Algeria and Nigeria, therefore we focus on the area above those major emissions sources and in the downwind areas of the eastern Tropical Atlantic. For the averaged LIVAS profiles we used nighttime profiles contained in a rectangular bounded between the 11.5^{o}N and 35.55^{o}N parallels and stretched between the 25.5^{o}W and 12.5°E meridians. We have modified the revised manuscript accordingly in lines 417, page 14 and we have also included a third plot in Fig. 9 (Fig10 in the original manuscript) in line 943, page 38, to depict clearly the selected area of interest:

"The mean LIVAS profile is provided by averaging the night-time profiles over the region between 25.5°W to 12.5°E and 11.5°N to 35.5°N, during 5 to 25 August 2015. This area includes the main dust sources that affected the vicinity of Cape Verde (Ryder et al., 2018) and the region of the dust outflow over the Ocean, as well."

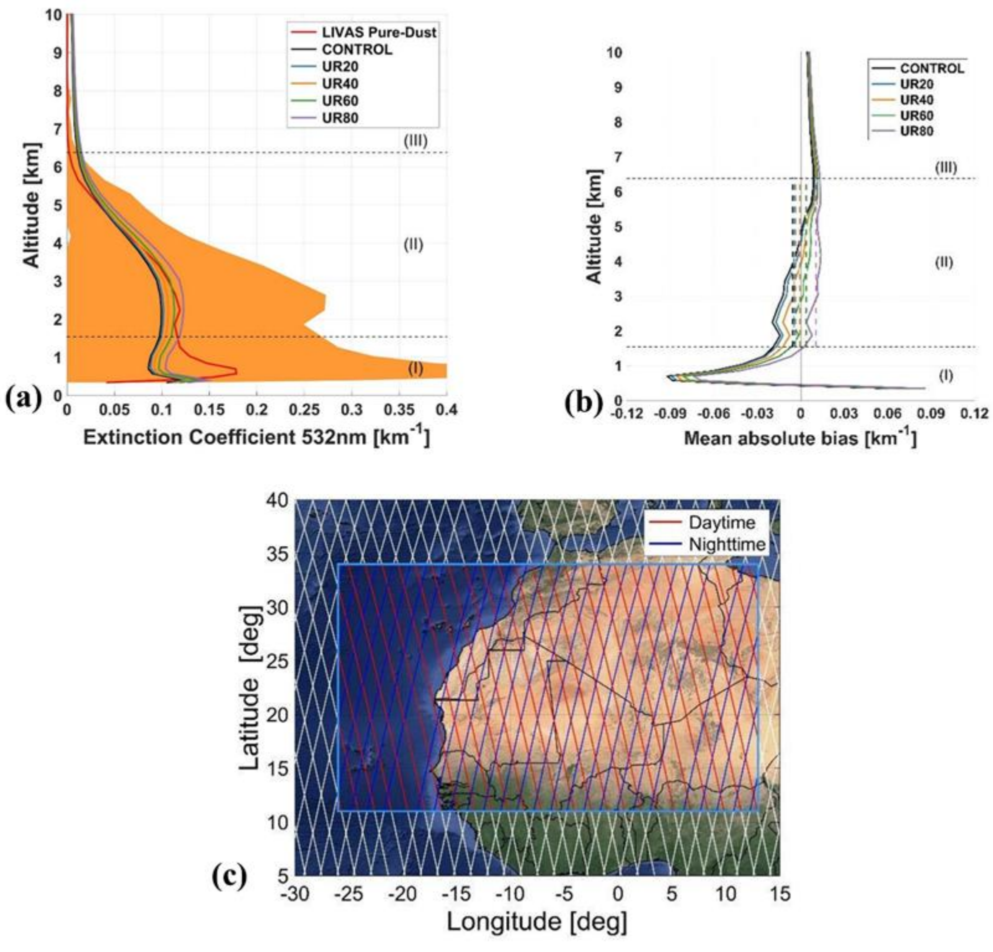

Figure 9: (a) Profile of the mean extinction coefficient at 532 nm, by LIVAS pure-dust product (black red line), and profiles of the mean extinction coefficient at 532 nm simulated from the different experiments of Table 3 (CONTROL, UR20/40/60/80). The orange shading indicates the standard deviation of the LIVAS profile averaging. (b) The mean absolute biases between the LIVAS profile and the simulated profiles from the different experiments, in the domain of interest, between 05/08/2015 and 25/08/2015. The vertical dashed lines are the mean absolute bias between the LIVAS profile and the simulated profiles from the different experiments averaged over the altitudes of region II. (c) The domain of interest and the daytime (red) and nighttime (blue) CALIPSO overpasses. The

vertical dashed lines are the mean absolute bias between the LIVAS profile and the simulated profiles from the different experiments averaged over the altitudes of region II.

Lines 397 and 830: the Livas pure-dust product is illustrated with the red line.

Done.

Line 423: "… 0.066 m/s for particles with D between 5.5 and 17 μm … " according to line 390.

Done

Line 428: "… compared to this study …".

Done

Lines 438, 457, 461, 468: "Mallios et al. (2021)" because there is no Mallios et al. 2021a or Mallios et al. 2021b in the References section.

done

Line 476: "… asphericity …".

Done

Line 781: "… b932 and b934 are also …".

Done

Figure 3: are the symbols of each flight below its maximum height necessary? They are hidden by the symbol of the highest flight of each run. The other information (flight number, run, height) must remain. Moreover, some runs of figure 9b (b924_R04, b928_R02, b932_R02, b934_R04) and figure 8 (b928_R02) are not included in figure 3, while b932_R05 appears in figure 3, but not in figure 9b.

We would like to thank the reviewer for pointing out the missing flight RUNS. Thanks to that comment we realized that we erroneously have ignored the flight segments b928 R10, R11 and R12. The inclusion of those flights change also Figure 8 of the revised manuscript (Figure 9 in the original manuscript). In the revised Fig. 3 we added the missing names of flight b928. Additionally, we improved the presentation of the flight tracks. In the revised Fig.3 the flight tracks of each flight RUN, are depicted separately, along with the model points that are used for the collocation procedure between model and observations. The revised plot is inserted in lines 903, page 32:

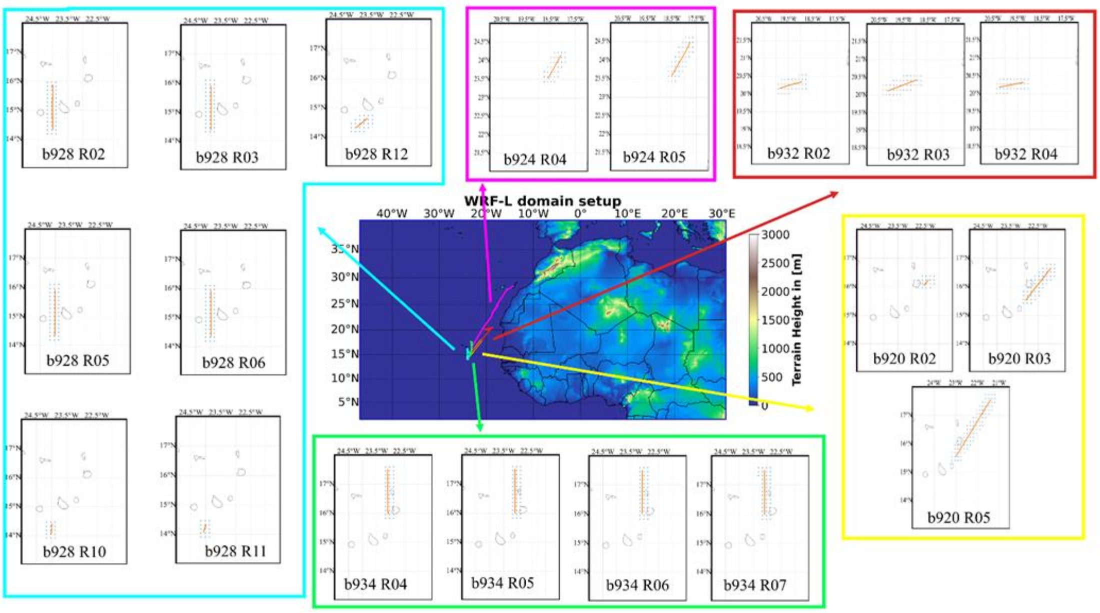

Figure 3: Domain and topography map of the WRF-L model simulations, with a horizontal grid spacing of 15km, and 70 vertical levels. The tracks of the AER-D flights, used in this study (b920, b924, b928, b932 and b934), are depicted in the central plot with different

colors. In the surrounding maps, the orange dots indicate the aircraft tracks of each flight RUN. The blue dots correspond to the collocated model grid points. "

Line 817: please clarify how were the uncertainties calculated? At what significance level?

We would like to thank the reviewer for the useful comment. The vertical bars in Figure 7 (Figure 8 in the original manuscript) refer to the total (random and systematic) measurement error. A full description of these errors is included in Ryder et al. (2018). Based on our reply we have modified accordingly Section 2.2.1 of the revised manuscript in line 277, page 10:

*"We also use PSD observations during horizontal flight legs at a constant height (referred either as RUNs or flight segments) over the Atlantic Ocean during AER-D. We use measurements taken with PCASP (D =0.12-3.02 μm) for fine dust particles. For the coarse and giant mode of dust we used measurements from CDP (D=3.4-20 μm, although CDP measurements availability extends up to 95.5 μm as it is explained below) and the two-*dimension Stereo probe *(2DS, D = 10–100 μm -although the instrument measures up to 1280 μm few particles larger than 100μm were detected). For the light scattering techniques of PCASP and CDP, a RI = 1.53-0.001i is assumed for the conversion of the optical to geometric diameter (as in FENNEC 2011 campaign). CDP observations extend up to the size of 95.5 μm, thus data from CDP and 2DS partly overlap in their size range. Since 2DS observations are more reliable in the overlapping size range, we used the CDP observations for particles with sizes up to 20 μm. Also, 2DS-XY observations are preferred over the 2DS-CC, since they better represent the non-spherical particles. A more detailed description of the in-situ instruments and the corresponding processing of the data acquired during the AER-D campaign is included in Ryder et al., (2018). The error bars represent the total (random and systematic) measurement error due to the counting error, the discretization error, the uncertainties in the sample area and the uncertainties in the bin size due to Mie singularites (Ryder et al., 2018). All PSD measurements are at ambient atmospheric conditions. The locations of the flights of AER-D used in this study are depicted in Fig.3."*

In the discussion of Figure 7 in line 367, page 13

Figure 7 illustrates the simulated PSDs, from each experiment (i.e., CONTROL and URx), along with those acquired by the airborne in situ measurements at different segments and altitudes of the flight b928 in the surrounding area of Cape Verde (downwind region). For the other AER-D flights (i.e., b920, b924, b932 and b934) similar findings are drawn and for brevity reasons are omitted here and are included in the supplementary material (Fig.S4). All AER-D measurements demonstrate the impacts of the processes that are associated with dust transport. The red squares correspond to the observations and the error bars represent the total (random and systematic) measurement error (see Sect 2.2.1)."

And also the caption of Fig. 7 in lines 925, page 36:

"***Figure 7: Modeled and observed dust PSD of flight b928, over the Atlantic Ocean during AER-D, for straight-level-runs (a) R02, (b) R03, (c) R05, (d) R06, (e) R10, (f) R11 and (g) R12. The in situ observations are shown with red squares (along with the total measurement error). The collocated modeled PSDs are shown with lines, for the CONTROL run (black), UR20 (blue), UR40 (orange), UR60 (green), and UR80 (purple) and the corresponding standard deviation with the associated error bars. The brown vertical lines indicate the limits of the model size bins. The inlet maps show the flight segment track and the collocated model grid points.***"

Line 825: please add b928_R02.

Done

Line 834: please add in the caption what are the vertical dashed lines in region II.

We have revised the caption of Fig. 9 accordingly (Fig.10 in the original manuscript), by including the description of the vertical dashed lines in line 944, page 38 of the revised document:

"Figure 9: (a) Profile of the mean extinction coefficient at 532 nm, by LIVAS pure-dust product (black red line), and profiles of the mean extinction coefficient at 532 nm simulated from the different experiments of Table 3 (CONTROL, UR20/40/60/80). The orange shading indicates the standard deviation of the LIVAS profile averaging. (b) The mean absolute biases between the LIVAS profile and the simulated profiles from the different experiments, in the domain of interest, between 05/08/2015 and 25/08/2015. The vertical dashed lines are the mean absolute bias between the LIVAS profile and the simulated profiles from the different experiments averaged over the altitudes of region II. (c) The domain of interest and the daytime (red) and nighttime (blue) CALIPSO overpasses. The vertical dashed lines are the mean absolute bias between the LIVAS profile and the simulated profiles from the different experiments averaged over the altitudes of region II."

Table 2: The MM5 surface layer scheme is 1 or 91 in WRF 4.2.1, but not 2.

We would like to thank the reviewer for pointing this out. We agree with the reviewer's comment. In the model configuration we used the Monin-Obukov-Janjic (Janjic, 2019) surface layer scheme. Therefore, we revised Table 2 accordingly in line 957, page 39 of the revised manuscript.

Table 2 Configuration parameters of the WRF-L runs

Parameterization	***Scheme***	***Parameterization***	***Scheme***
Surface Model	*Noah (Chen and Dudhia, 2001)*	*sf_surface_physics*	*2*
Surface Layer	*Monin-Obukov-Janjic* (Janić, 2001)	*sf_sfclay_physics*	*2*
Radiation (SW and LW)	*RRTMG (Iacono et al., 2008)*	*ra_sw(lw)_physics*	*4*
Microphysics	*Morrison 2-moment (Morrison et al., 2005)*	*mp_physics*	*10*
Cumulus	*Grell-3 (Grell and Dévényi, 2002)*	*cu_physics*	*5*
Boundary Layer	*MYNN 2.5 (Nakanishi and Niino, 2006)*	*bl_pbl_physics*	*5*
Chemistry	*GOCART simple (Ginoux et al., 2001; LeGrand et al., 2019)*	*chem_opt*	*300*
Dust Scheme	*AFWA (LeGrand et al., 2019)*	*dust_opt*	*3*

References

Danielson, J. J. and Gesch, D. B.: Global multi-resolution terrain elevation data 2010 (GMTED2010)., 2011.

Gilliam, R. C. and Pleim, J. E.: Performance Assessment of New Land Surface and Planetary Boundary Layer Physics in the WRF-ARW, J. Appl. Meteorol. Climatol., 49(4), 760–774, doi:10.1175/2009JAMC2126.1, 2010.

Ryder, C. L., Marenco, F., Brooke, J. K., Estelles, V., Cotton, R., Formenti, P., McQuaid, J. B., Price, H. C., Liu, D., Ausset, P., Rosenberg, P. D., Taylor, J. W., Choularton, T., Bower, K., Coe, H., Gallagher, M., Crosier, J., Lloyd, G., Highwood, E. J. and Murray, B. J.: Coarse-mode mineral dust size distributions, composition and optical properties from AER-D aircraft measurements over the tropical eastern Atlantic, Atmos. Chem. Phys., 18(23), 17225–17257, doi:10.5194/acp-18-17225-2018, 2018.

Gkikas, A. and NOA team: Assessing the impact of Aeolus wind data assimilation on the numerical simulations of Saharan dust outflows towards the Tropical Atlantic Ocean, Aeolus 3rd Anniversary Conference,28/3/2022-1/4/2022, Taormina , Italy.